Regulation of Cell Division Cycle Progression by *bcl*-2 Expression: A Potential Mechanism for Inhibition of Programmed Cell Death

By Svetlana Mazel,* Douglas Burtrum,* and Howard T. Petrie*‡

*From the Immunology Program, *Memorial Sloan Kettering Cancer Center and ‡Cornell University Graduate School of Medical Sciences, 1275 York Avenue, New York, NY 10021 U.S.A.*

Summary

Expression of the *bcl*-2 gene has been shown to effectively confer resistance to programmed cell death under a variety of circumstances. However, despite a wealth of literature describing this phenomenon, very little is known about the mechanism of resistance. In the experiments described here, we show that *bcl*-2 gene expression can result in an inhibition of cell division cycle progression. These findings are based upon the analysis of cell cycle distribution, cell cycle kinetics, and relative phosphorylation of the retinoblastoma tumor suppressor protein, using primary tissues in vivo, ex vivo, and in vitro, as well as continuous cell lines. The effects of *bcl*-2 expression on cell cycle progression appear to be focused at the G_1 to S phase transition, which is a critical control point in the decision between continued cell cycle progression or the induction programmed cell death. In all systems tested, *bcl*-2 expression resulted in a substantial 30–60% increase in the length of G_1 phase; such an increase is very substantial in the context of other regulators of cell cycle progression. Based upon our findings, and the related findings of others, we propose a mechanism by which *bcl*-2 expression might exert its well known inhibition of programmed cell death by regulating the kinetics of cell cycle progression at a critical control point.

The *bcl*-2 gene was discovered by virtue of its location at the breakpoint of the t(14;18) chromosomal translocation found in most human follicular lymphomas (1). Since that time, *bcl*-2 expression has been shown to confer a resistance to programmed cell death (PCD)[1] in a variety of systems, including growth factor withdrawal from hematopoietic cell lines (2), corticosteroid or antibody-induced thymocyte ablation in vivo (3, 4), and oncogene transfection of cell lines (5, 6). Although Bcl-2 has been proposed to function by a variety of means, including protection from oxidative damage due to cellular metabolism (7), or through the inhibition of activators of the cell death program such as *bax* or ICE (8), the mechanism of this resistance remains unclear.

It is becoming clear that many proteins that can induce PCD are in fact components of the cell division cycle, and that the cell cycle and PCD are inextricably linked (for a review see reference 9). Most conspicuously, expression of c-*myc* has been shown to initiate both proliferation and PCD in vitro (10). Interestingly, the same regions of the Myc protein known to be required for the more conventional consequences of Myc expression (i.e., mitogenesis) were required for the induction of PCD. Expression of the homeobox fusion gene E2A-PBX1 (resulting from a t(1;19) chromosomal translocation in certain human leukemias) can also induce both proliferation and PCD in vivo (11). Expression of the tumor suppressor protein retinoblastoma (pRb), a known regulator of cell cycle progression, has been shown to repress PCD induced by radiation (12). Enforced expression of the transcription factor E2F1 (a primary target of pRb) leads to inappropriate S phase entry and incomplete DNA synthesis, which is terminated by PCD (13). Another tumor suppressor gene, p53, has been shown to be capable of the induction of PCD (14), possibly through inducing the transcription of *bax* (15), a known positive regulator of PCD (16). Senescent fibroblasts also upregulate many cell cycle related genes, such as c-*fos*, c-*myc*, c-*jun*, and cdc2, prior to undergoing PCD (17); similar upregulation of proliferating cell nuclear antigen (PCNA), c-*myc*, p53, cyclin A, and cdc2 has been observed in cell lines induced to undergo PCD (18). In another study, two primary catalytic partners of cyclin A (cdc2 and cdk2) have been shown to be activated in cell lines induced to undergo PCD (19). These and many other studies thus establish a

[1] *Abbreviations used in this paper:* BrdU, 5-bromo-2′-deoxyuridine; CAS, concanavalin A supernatant; DPBS, Dulbecco's phosphate-buffered saline solution; LN, lymph node; PCD, programmed cell death; PE, phycoerythrin; PI, propidium iodide; pRb, protein retinoblastoma.

 J. Exp. Med. © The Rockefeller University Press • 0022-1007/96/05/2219/08 $2.00
Volume 183 May 1996 2219–2226

strong intellectual linkage between PCD and the cell division cycle.

In the experiments presented here, we demonstrate that *bcl*-2 gene expression can regulate progression of the cell cycle, in both primary tissues (in vivo and in vitro) and in continuous cell lines. In addition, we propose a model to reconcile these findings with the known effects of *bcl*-2, especially the inhibition of PCD. Together, these data should help to elucidate the means by which *bcl*-2 inhibits PCD, and further provide insights into the relationship between PCD and cell division in both normal and malignant cells.

Materials and Methods

Mice. Mice expressing a lymphoid-restricted human *bcl*-2 transgene construct were generated as described (4), and have since been extensively backcrossed onto the C57BL/6 background (B6/*bcl*-2). C57BL/6 and B6/*bcl*-2 transgenic mice used in the experiments described here were littermates from the mating of C57BL/6 mice (Jackson Laboratories, Bar Harbor, ME) with B6/*bcl*-2 heterozygotes.

Surface Immunophenotyping and Cell Sorting. These procedures were performed as previously described (20).

Bromodeoxyuridine Administration and Analysis. 5-bromo-2′-deoxyuridine (BrdU; Sigma, St. Louis, MO) was prepared fresh daily, and was administered at 0.8 mg/ml in the drinking water. No adverse affects of this treatment (e.g., weight loss or thymic atrophy) have been observed, in agreement with the published findings of others (21). Following the appropriate feeding interval, thymuses were harvested and stained with anti-CD4 conjugated to phycoerythrin (PE) and anti-CD8 conjugated to biotin, followed by CyChrome streptavidin (PharMingen, San Diego, CA), to allow the identification of $CD4^-8^-$ or $CD4^+8^+$ cells. Stained cells were washed and fixed for 72 h at 4°C using 1% paraformaldehyde/0.01% Tween-20 in Dulbecco's phosphate-buffered saline solution, pH 7.2 (DPBS). Following washing in DPBS, fixed cells were treated for 90 min at 37°C with DNAse I (50 U/ml) in a solution of 10 mM HCl/4.2 mM $MgCl_2$/150 mM NaCl. Cells were again washed in DPBS, stained with FITC-conjugated anti-BrdU antibody (Becton-Dickinson, Mountainview, CA), and analyzed on a FACScan® (Becton-Dickinson).

In vitro T Cell Activation. Lymph node (LN) T cells were prepared from pooled axillary and brachial LN from C57BL/6 or B6/*bcl*-2 mice by two sequential rounds of B cell depletion using anti-immunoglobulin-coated Dynabeads (Dynal, Oslo, Norway). T cells prepared in this fashion were >95% pure, as assessed by flow cytometry using anti-TCR antibody (not shown). 24-well tissue culture trays were coated with purified anti-TCR-β antibody (clone H57-597; Caltag Laboratories, South San Francisco, CA) by incubation for 1 h at 37°C in DPBS containing antibody at 25 μg/ml, followed by washing with DPBS. Purified T cells were resuspended at 1.2×10^6 cells/ml in RPMI 1640 medium containing 10% FBS, 2 mM glutamine, 5×10^{-5} M β-mercaptoethanol, and 10% rat concanavalin A supernatant (CAS). 1 ml of cells per well was dispensed into anti-TCR-coated trays, as above. Cells were harvested after the appropriate interval, assessed microscopically for cell number and viability, and fixed and analyzed as described below.

DNA Content/Cell Cycle Distribution Analysis. For DNA content analysis only, cells were washed in DPBS, resuspended in 50 μl of DPBS, slowly added to 1 ml of ice-cold 70% ethanol, and stored overnight at 4°C. After this fixation step, cells were centrifuged and resuspended in 2 N HCl/0.5% Triton X-100 in H_2O for 30 min at room temperature. After denaturation, cells were again centrifuged and resuspended in 0.1 M $Na_2B_4O_7$, pH 8.5, to neutralize the acid. Cells were washed in DPBS/5% FBS/0.5% Tween-20 and resuspended in propidium iodide (PI, 5 μg/ml in DPBS) for at least 2 h before analysis on a FACScan® (Becton-Dickinson). For DNA content analysis and simultaneous BrdU quantitation, cells were stained with FITC-conjugated anti-BrdU (Becton-Dickinson) prior to the addition of PI/DPBS, as above.

Cell Lines and In Vitro BrdU Labeling. FDC-P1 cells infected with a retroviral construct containing the human *bcl*-2 gene or a control retroviral construct were generated as described (2). Both lines were grown in Dulbecco's Modified Eagles Medium (DMEM) containing 10% FBS, recombinant IL-3 (22), and selective antibiotics (G418, 500 mg/ml; Sigma); selective medium was removed for 3–4 cell divisions before the initiation of experiments. Both control and *bcl*-2-expressing cell lines were periodically and routinely subcloned by limit dilution. To minimize the effects of culture differences and to maximize culture integrity, cells were passaged every 12 h for several days before use for experimentation. Pulse labeling with BrdU was accomplished by addition of BrdU to a final concentration of 10 μM, followed by incubation for 40 min under normal culture conditions, and subsequent resuspension of labeled cells in conditioned medium without BrdU. After the appropriate intervals, cells were fixed and stained as described above.

Protein Immunoblot Analysis. Cells were washed twice in DPBS containing 20 mM EDTA (DPBSE). Following the second wash, cell pellets were lysed for 5 min at 96°C using a solution of 62.5 mM Tris, pH 6.8/700 mM β-mercaptoethanol/10% glycerol/2.3% SDS/0.001% bromophenol blue (4×10^7 cells/ml). Extracts were cooled on ice, and DNA was sheared by 3–4 passages through a 28-gauge needle. Extracts were centrifuged at 45,000 *g* for 20 min to remove insoluble material, and the supernatants were electrophoresed on 7.5% acrylamide minigels (7.3 × 8 cm) using 25 mM Tris/192 mM glycine/0.1% SDS buffer. Gel lanes were loaded with equivalent volumes of cell extracts (generally 4×10^5 cell equivalents/lane). Nuclear extracts from PMA-treated NIH/3T3 cells (Santa Cruz), or extracts from FDC-P1 cells 3 h after release from an M phase block (Nocodazole, 40 μg/ml; Sigma) were included as pRb controls where appropriate. After electrophoresis, the proteins were transferred to nitrocellulose membranes (HyBond ECL; Amersham, Arlington Heights, IL) using a Mini Trans-Blot apparatus (Bio-Rad, Hercules, CA) according to the manufacturers instructions. Membranes were immunoblotted with rabbit polyclonal antibody to pRb (no. SC-50; Santa Cruz Biotechnology, Santa Cruz, CA) followed by HRP-conjugated goat anti–rabbit IgG (Santa Cruz) according to the manufacturers recommendations. Immunoblots were visualized using ECL detection (Amersham) according to the manufacturers recommendations. The film images were scanned using a laser scanning densitometer (Bio-Rad); quantitative analysis of the scanned images was performed using Molecular Analyst software (Bio-Rad).

Statistics. Statistical differences were analyzed where appropriate using the Student's two-tailed *t* test for independent samples.

Results

The Kinetics of In Vivo DNA Labeling in Normal and bcl-2 Transgenic Littermate Mice. The results of in vivo labeling of thymocyte DNA, using continuous BrdU feeding and anti-BrdU antibodies, are shown in Fig. 1. Since thymus

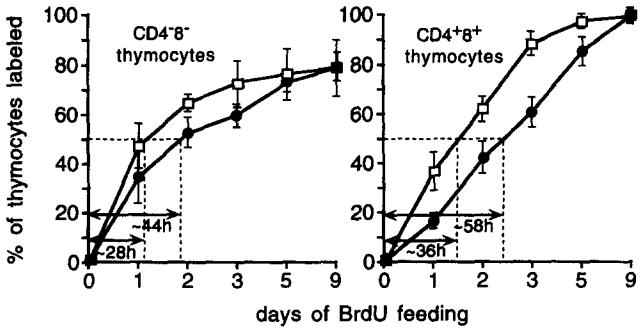

Figure 1. The kinetics of in vivo labeling of thymocyte DNA in *bcl-2* transgenic or control mice. Transgenic or control mice were fed BrdU in the drinking water for the periods indicated, followed by immunofluorescent staining of thymocytes for surface CD4/8 and nuclear BrdU and flow cytometry. Both $CD4^-8^-$ cells (most of which are dividing) and $CD4^+8^+$ cells (most of which have stopped dividing) were slower to label in *bcl-2* transgenic mice (solid circles) than in control littermates (*open squares*). The differences in time until half-maximal labeling are indicated by hatched vertical lines, and represent an ~60% time lag in transgenic cells, regardless of developmental stage. Differences were statistically significant ($P < 0.05$) at all logarithmic phases of labeling. Data points represent the arithmetic mean ± standard deviation for at least three experiments.

size, thymic subset ratios, and T cell surface markers expression (including CD3/TCR) are indistinguishable between *bcl-2* transgenic mice and their non-transgenic littermates (4), the direct assessment of isogenic *bcl-2* expression can be made both in vivo and in vitro. The labeling pattern for $CD4^-8^-$ cells was essentially log phase, and that of $CD4^+8^+$ essentially linear, in both types of mice, as expected for dividing and non-dividing populations, respectively (23). Further, both $CD4^-8^-$ and $CD4^+8^+$ cells ultimately labeled to the same maximal level in both types of mice. These findings again demonstrate the general developmental equity between transgenic and control animals (4). Nonetheless, a substantial lag in DNA labeling, representing an approximate 60% increase in the time required before half-maximal labeling, was found in *bcl-2* transgenic thymocytes. The *bcl-2*-induced delay in DNA labeling was consistent in both the largely dividing $CD4^-8^-$ cells and in their mostly non-dividing $CD4^+8^+$ progeny (Fig. 1). These results show that the singular expression of a *bcl-2* transgene can profoundly affect thymocyte turnover, resulting in an ~60% increase in the time required for comparable levels of DNA synthesis (i.e., cell division) in transgenic mice.

Relative Cell Cycle Distribution of Thymocytes from Normal or bcl-2 Transgenic Littermate Mice. Healthy dividing cells possess a variable amount of nuclear DNA, ranging from the normal ($2n$) amount found in most somatic cells, up to twice that amount ($4n$) in cells preparing to undergo mitosis. Measurement of the DNA content profile in a given population of cells can thus provide an estimate of the relative cell division status; again, the similarities in thymocyte cell number and subset ratio allow a direct comparison between *bcl-2* transgenic and non-transgenic mice (4). The results of this type of analysis, using purified $CD4^-8^-$ or $CD4^+8^+$ thymocytes, are shown in Fig. 2. Thymocytes from *bcl-2* transgenic mice showed significantly ($P < 0.05$) more cells with $2n$ DNA content (i.e., G_0/G_1 stage of cycle), and proportionally fewer cells in S phase; no differences ($P > 0.1$) were observed in the frequency of cells with 4n DNA content (G_2/M phases). Statistically significant differences in the G_1 and S phase distributions were observed in $CD4^+8^+$ as well as $CD4^-8^-$ cells; differences in the former finding are even more striking when one considers that only a small proportion (~10%) of these cells are dividing. These findings add further support to the concept that *bcl-2* gene expression may affect the thymocyte cell division cycle, and provide additional evidence to suggest that this effect is directed towards the G_1/S phase transition.

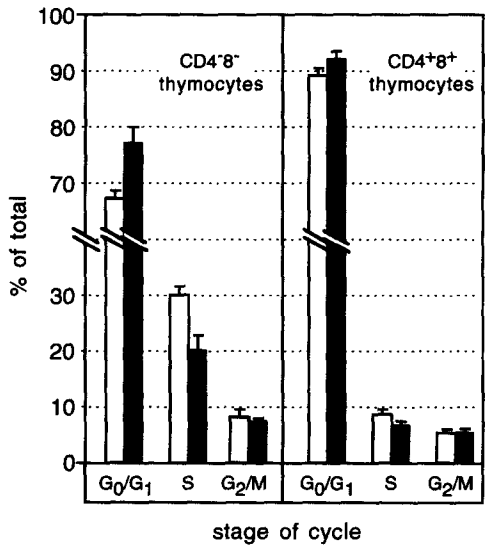

Figure 2. Cell cycle distribution of ex vivo thymocytes from *bcl-2* transgenic or control mice. $CD4^-8^-$ and $CD4^+8^+$ thymocytes were prepared from transgenic or control mice by cell sorting. The DNA content of sorted cells was analyzed by propidium iodide staining and flow cytometry. In both cases, cells from *bcl-2* transgenic mice (*solid bars*) had more cells in G_0/G_1 phase, and proportionally fewer cells in S phase, than their normal littermates (*open bars*); these differences were statistically significant ($P < 0.05$). No differences in the proportions of M phase cells were observed ($P > 0.1$). Data points represent the arithmetic mean ± standard deviation for at least three experiments.

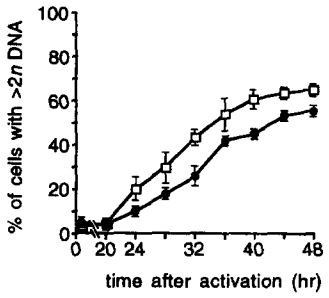

Figure 3. T cells from *bcl-2* transgenic or control mice after in vitro stimulation; the kinetics of entry into S phase. T cells were purified from the lymph nodes of transgenic or control mice, and stimulated to proliferate using immobilized anti-TCR antibody and cytokines. At the appropriate intervals, cultures were harvested, and cell cycle status was analyzed by propidium iodide staining of DNA and flow cytometry. T cells from *bcl-2* transgenic mice (*solid circles*) were slower to enter S phase than the equivalent cells from control mice (*open squares*); the differences were statistically significant ($P < 0.02$). Data points represent the arithmetic mean ± standard deviation for three to four experiments.

The Kinetics of Cell Cycle Progression in bcl-2 Transgenic or Control T Cells Activated In Vitro. Peripheral T lymphocytes from the LN of both *bcl*-2 transgenic and normal animals are mostly resting cells with 2*n* DNA content. Using anti-TCR-coated plastic trays and cytokines, resting T cells (G_0) can be activated in vitro, an event which is followed by DNA synthesis and cell division. The rate of this transition can be monitored through kinetic analysis of cellular DNA content, as described in the preceding section. The results of such analyses are shown in Fig. 3. Activated cultures of LN T cells from *bcl*-2 transgenic mice were slower to move out of G_0/G_1 phases of cycle, and proportionally slower to move into S phase. The differences between *bcl*-2 transgenic and control cultures were statistically significant ($P < 0.02$) at all times points where proliferation could be detected (i.e., 24 h and onward). Experiments were terminated at 48 h, before the occurrence of any cell division and concomitant reversion to the 2*n* stage. Since the in vitro response of T cells from *bcl*-2 transgenic mice is even more robust than that of T cells from normal mice (4), these differences in the kinetics of cell cycle progression are even more profound. Thus, these experiments provide additional evidence that *bcl*-2 gene expression can inhibit progression of the cell division cycle. Further, these in vitro experiments eliminate the possibility that feedback inhibition due to prolonged $CD4^+8^+$ cell survival was responsible for the observed inhibition of thymocyte cell division in *bcl*-2 transgenic mice (Figs. 1 and 2), since homeostatic controls are not in effect in culture. Additional evidence for this finding is provided in the next section.

Effects of Ectopic bcl-2 Gene Expression on Cell Cycle Progression in Continuous Cell Lines. To support the results obtained using primary tissues from *bcl*-2 transgenic and control mice (Figs. 1–3), defined in vitro systems were sought. Isogenic FDC-P1 myelocytic cell lines expressing *bcl*-2-containing or control retroviral constructs have been described previously

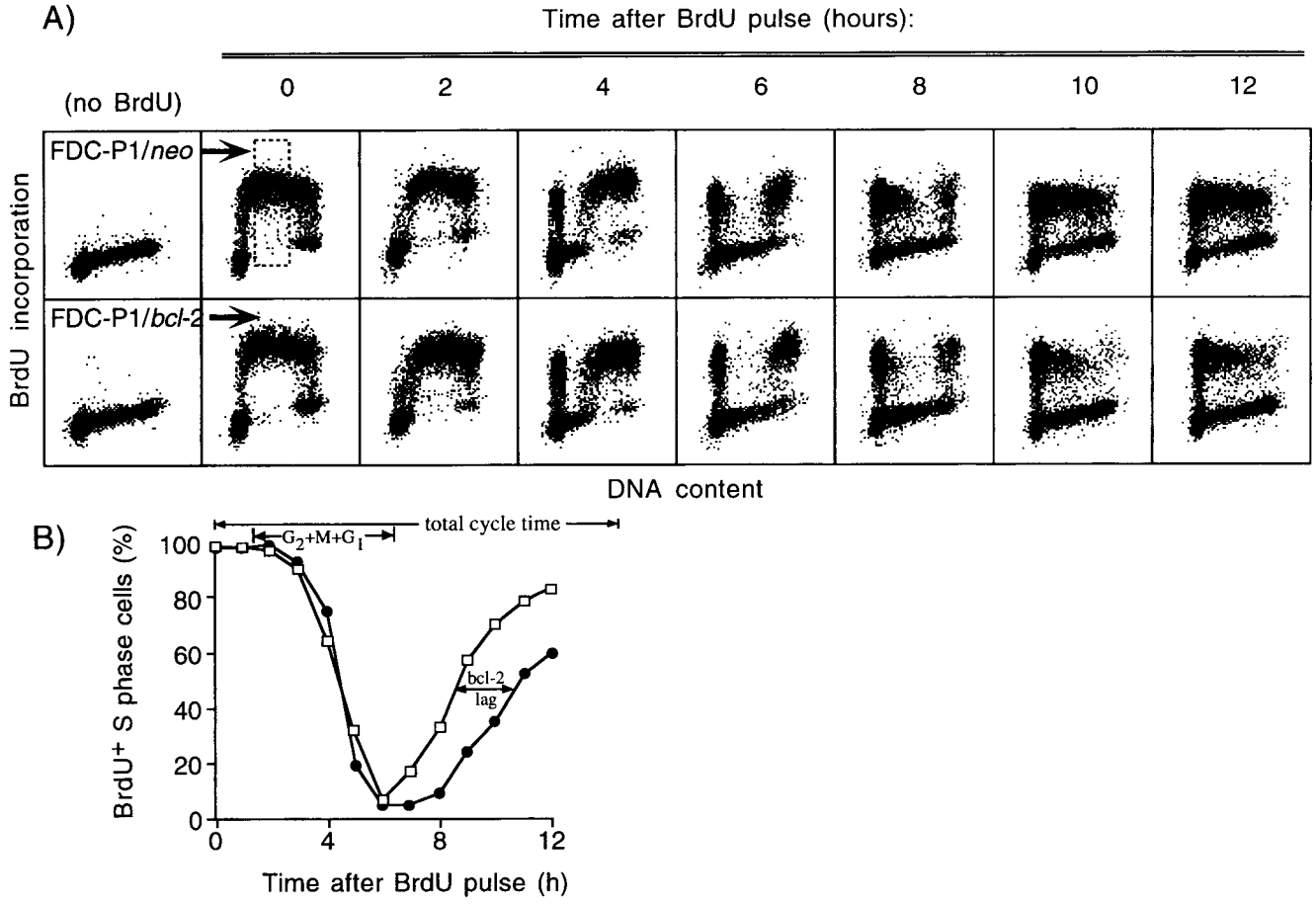

Figure 4. Kinetics of progression of *bcl*-2-expressing or control cells through the stages of cell cycle. S phase cells from *bcl*-2-expressing or control FDC-P1 cultures were labeled using a 40-min pulse of BrdU. The transit of labeled cells through the cell cycle was followed by simultaneous analysis of BrdU incorporation and DNA content using flow cytometry. Cells expressing *bcl*-2 (*A*, lower series) moved into G_2, M, and G_1 phases of cell cycle at the same rate as controls (upper series). However, the reentry of labeled cells into S phase (beginning at 6 h in controls) is delayed in *bcl*-2 expressing cells. *B* graphically depicts this effect, by comparing the rate of exodus and subsequent reentry of $BrdU^+$ cells through S phase (defined by the hatched area marked in *A*, time 0 control); both cell types moved out of S phase at the same rate, but reentry was delayed in bcl-2^+ cells (solid circles). The approximate times for complete cell cycle (~14 h), G_2 + M + G_1 phases (~6 h), and the *bcl*-2-induced lag in S phase reentry (~2 h) are indicated. Data points represent the pooled arithmetic mean for two experiments.

(2); thus, the direct assessment of ectopic *bcl*-2 gene expression can be compared in the absence of other contributing factors. Using a 40-min pulse of BrdU, we followed the progression of an essentially synchronous population of S phase cells throughout the phases of cell cycle, as measured by DNA content analysis (Fig. 4). Both *bcl*-2-expressing and control FDC-P1 cells labeled with BrdU to approximately the same extent during the pulse (*A*, time 0 h); this finding attests to the initial good health of the two starting populations, since they have just passed the G_1 to S phase checkpoint. The analysis of labeled cells through a single cell cycle ensures that minimal DNA damage and cell death can occur, and eliminates the possibility that any delay in cell cycle progression simply represents prolonged survival of damaged or dying cells by *bcl*-2. The progression of both types of cultures out of S phase, and into first G_2/M (4*n* DNA content), and then G_0/G_1 (2*n* DNA content), is the same (2–6 h). However, the reappearance of $BrdU^+$ cells into S phase is slower in *bcl*-2-infected cells than in control cells, as can be seen beginning at 6 h. The results are graphically represented in panel B, by plotting the exodus of BrdU-labeled (i.e., S phase) cells out of and then back into S phase; exodus is identical in both cell types, while reentry is delayed in *bcl*-2 infected cells. Since the transit from S phase through G_2/M and into G_1 is the same in both types of cells (*A* and *B*, 0–6 h), the differences in the kinetics of reentry into S phase must occur at the G_1/S phase transition. The G_1 phase of cell cycle in FDC-P1 controls is ~5 h (Fig. 4 *A*, and additional data not shown). Thus, the lag induced by *bcl*-2 (~2 h) increases the length of G_1 by ~40%, a value consistent with the delay found using the in vivo labeling system described above (Fig. 1). Such an increase must be considered to be very substantial in biological terms; by comparison, multiple ectopic expression of the predominant G_1 cyclins D2 and D3 only changes the length of G_1 by 28% in a similar system (23). The data shown in Fig. 4 thus provide a clear demonstration of the inhibition of cell cycle progression by *bcl*-2, at precisely the stage of cell cycle which is critical to the decision between continued cell division or the induction of PCD (i.e., the G_1/S transition). Further, these experiments demonstrate that such inhibition is not limited to thymocytes or even lymphocytes, but is apparently a pervasive effect in response to *bcl*-2 expression.

Differential Phosphorylation of Rb Associated with bcl-2 Gene Expression. The regulation of mammalian cell cycle progression has been extensively studied in recent years. In particular, many insights have been gained in regard to the G_1/S phase transition (25). One of the key regulators of this transition is the retinoblastoma protein, pRb. Phosphorylation of pRb (pRb-P) leads to the liberation of key transcription factors required for DNA synthesis, whereas dephosphorylation is generally representative of cell division cycle arrest before or near the G_1/S restriction point (25). Thus, the ratio of pRb-P to pRb can be used as a relative indication of cell cycle status. The results of pRb immunoblot analysis, using various *bcl*-2 expressing and control cells, are shown in Figs. 5 and 6. Control FDC-P1 cells express almost exclusively the phosphorylated form of pRb (Fig. 5, lane *3*), consistent with their extremely rapid cell division time of ~12–14 h (see Fig. 4); the ratio of pRb-P/pRb is ~4.1. FDC-P1/*bcl*-2 cells, on the other hand, express appreciable levels of the underphosphorylated forms of pRb (Fig. 5, lane *4*). The pRb-P/pRb ratio in these cells is ~2.5, nearly twofold less than that found in controls, consistent with a less rapid cell cycle status. Since the regulation of cell cycle progression through the G_1 restriction point by pRb is represented by a threshold, rather than a linear titration (25), a twofold increase is likely to represent a functional difference. In any case, even more profound differences in phosphorylation of pRb can be seen using ex vivo tissues from *bcl*-2 transgenic and control mice (Fig. 6), as discussed below.

Immature $CD4^-8^-$ thymocytes can be subdivided into several groups, which differ mainly with respect to the rearrangement status of their TCR-β loci (26). $CD24^+25^+44^{lo}$ $CD4^-8^-$ cells are slowly cycling and endogenous *bcl*-2^+; their immediate progeny ($CD24^+25^-44^{lo}$ $CD4^-8^-$ cells) are rapidly dividing and endogenous *bcl*-2^- (23, 26). Thus, the comparison of these two cell types from *bcl*-2 transgenic or control mice allows the clear assessment of the effects of *bcl*-2 expression on cell cycle status during normal cell de-

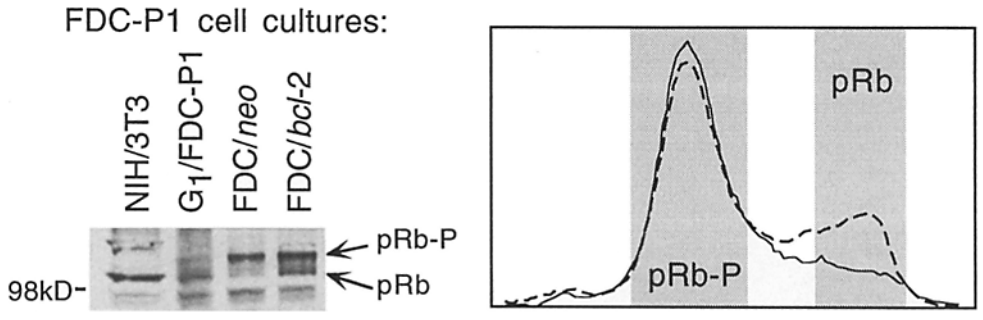

Figure 5. Relative pRb phosphorylation in continuous cell lines expressing ectopic *bcl*-2 genes or control vectors. Fig. 5 shows a pRb immunoblot analysis of *bcl*-2-expressing FDC-P1 cells and retrovirus-only controls. Lanes *1* and *2* (PMA-treated NIH/3T3 nuclear extracts, and early G_1-phase FDC-P1 extracts, respectively) show the normal location of underphosphorylated pRb. Asynchronous FDC-P1 controls expressed phosphorylated pRb (pRb-P) almost exclusively (lane *3*). Ectopic *bcl*-2 expression in these cells resulted in substantially higher levels of underphosphorylated pRb (lane *4*), consistent with a general decrease in cell cycle status. Histograms show scanning densitometry of the immunoblots; solid lines represent FDC-P1 control cultures, while hatched lines represent *bcl*-2-infected FDC-P1 cells. The shaded areas represent the approximate areas used for peak quantitation of phosphorylated and underphosphorylated pRb.

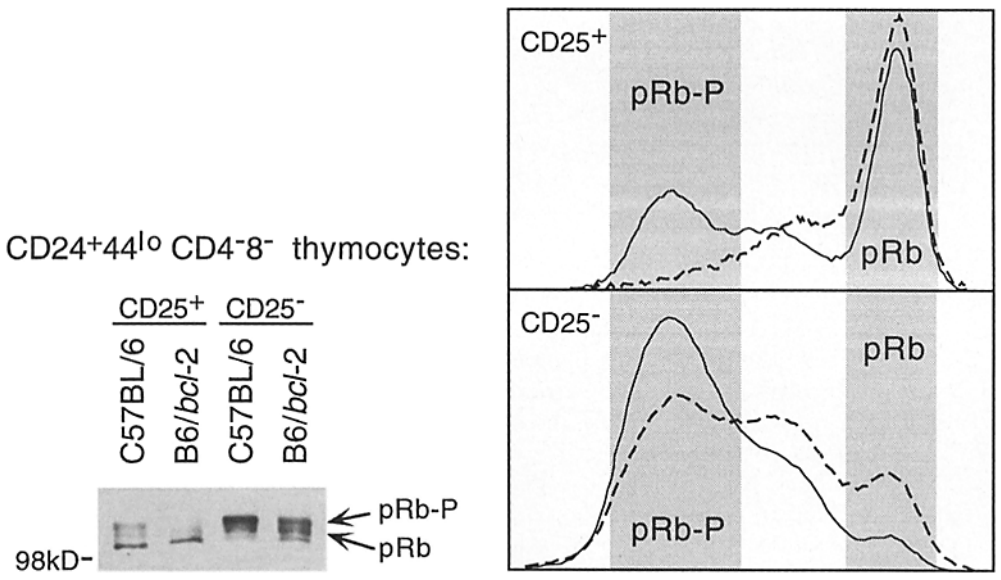

Figure 6. Relative pRb phosphorylation in purified subsets of thymocytes from *bcl*-2 transgenic or control mice. $CD24^+25^+44^{lo}$ $CD4^-8^-$ cells are slowly cycling and endogenous *bcl*-2^+; their immediate progeny ($CD24^+25^-44^{lo}$ $CD4^-8^-$ cells) are rapidly dividing and endogenous *bcl*-2^-. Immunoblot detection of pRb using extracts of such cells purified from *bcl*-2 transgenic or control mice are shown in Fig. 6. The more slowly dividing $CD25^+$ cells exhibit primarily the underphosphorylated form of pRb (lanes *1* and *2*); however, a detectable peak of phosphorylated pRb is also seen in control, but not transgenic, animals. The ratio of phosphorylated to underphosphorylated pRb is seven-fold higher in controls (see Results). After transition to the more rapidly cycling $CD25^-$ stage, a substantial shift in favor of pRb-P is seen (lanes *3* and *4*). However, the ratio of phosphorylated to underphosphorylated pRb is still four to five times higher in $CD25^-$ cells from control mice than in cells from *bcl*-2 transgenic mice. Histograms show scanning densitometry of the immunoblots; solid lines represent cells from control mice, while hatched lines represent cells from *bcl*-2 transgenic mice. The shaded areas represent the approximate areas used for peak quantitation of phosphorylated and underphosphorylated pRb.

velopment. The results of a pRb immunoblot analysis of such cells are shown in Fig. 6. $CD24^+25^+44^{lo}$ $CD4^-8^-$ cells (endogenous *bcl*-2^+) express mainly the underphosphorylated form of pRb in either transgenic or control mice (lanes *1* and *2*), consistent with their slowly dividing status. Nonetheless, a substantial peak representing phosphorylated pRb is evident in control mice (pRb-P/pRb = 0.7), as opposed to *bcl*-2 transgenic mice (pRb-P/pRb = 0.1), where essentially no pRb-P can be detected. Upon transit to the more rapidly dividing $CD24^+25^-44^{lo}$ $CD4^-8^-$ phenotype (endogenous *bcl*-2^-), a dramatic shift in favor of phosphorylated pRb is seen (lanes *3* and *4*). However, the ratio of phosphorylated to underphosphorylated pRb in control mice (pRb-P/pRb = 13.4) is four to five times higher than that found in the same cells from *bcl*-2 transgenic mice (pRb-P/pRb = 3.1). Again, this pattern of phosphorylation of pRb is consistent with a general decrease in the ability of cells to transit the G_1 restriction point in the presence of *bcl*-2 expression. This type of controlled analysis of defined *bcl*-2 transgene expression in the context of endogenous *bcl*-2 expression or repression, using well-characterized ex vivo tissues, thus provides very convincing evidence that *bcl*-2 expression can regulate cell cycle progression in a significant physiological fashion.

Discussion

A balance between cell division and cell death is an inherent event in the maintenance of homeostasis. Consequently, it is intellectually appealing to find that a single gene (i.e., *bcl*-2) may prove to be a central regulator in both of these processes. In recent years, a strong biochemical linkage between PCD and the cell division cycle has been emerging (see Introduction). Meanwhile, the molecular means by which *bcl*-2 expression can regulate PCD remains unresolved. Part of the mystery almost certainly results from a general failure to perceive PCD as a complex sequence of biochemical events, rather than as a fixed phenotype. Consequently, all of the proposed mechanisms, including a regulation of cell division cycle progression, may be found to play a role under the appropriate circumstances. In fact, the regulation of cell cycle progression by *bcl*-2 can be readily rationalized with the other proposed mechanisms for inhibition of PCD by *bcl*-2. For instance, retardation of G_1 to S phase progression by *bcl*-2 may provide the necessary time to repair DNA damage induced by oxidative metabolism, rather than preventing DNA damage per se. The involvement of *bcl*-2 antagonists, such as *bax*, may also be reconciled; for instance, p53 expression is stabilized by DNA damage, and p53 has been shown to be a positive regulator of *bax* transcription (15). It is important to emphasize that *bcl*-2 does not appear to affect the absolute magnitude of cell division in vivo, or to absolutely nullify the execution of cell division cycle. Rather, it appears that *bcl*-2 can affect the rate of cell cycle progression in a manner which may be sufficient to prevent the cell from undergoing PCD. In this light, it is informative to note that enforced expression of oncogenes associated with proliferation (such as c-*myc*) are sufficient to drive cells into PCD in a manner which can be inhibited by *bcl*-2 (5, 6).

A number of antagonists of *bcl*-2, such as *bax* and *bcl*-x_S have been described (reviewed in reference 8). The interactions of these with *bcl*-2 and *bcl*-2 homologues appears to occur in a stoichiometric fashion (8). Consequently, our studies cannot elucidate whether forced *bcl*-2 expression inhibits cell cycle progression directly, or rather indirectly through interaction with one of these other proteins. However, it is informative to note that repression of en-

dogenous *bcl*-2 expression and the onset of rapid cell division are coincident events, both during T cell development (26) and after peripheral T cell activation (27). In contrast, high level *bcl*-2 expression is found both in resting T and B lymphocytes and in their long-lived, slowly dividing thymocyte precursors (26). Therefore, differential regulation of *bcl*-2 appears be a prerequisite for cell cycle progression in lymphocytes. The finding that forced *bcl*-2 expression also inhibits cell cycle progression in a myelocytic cell line (Figs. 4 and 5) further supports a direct role for *bcl*-2 in the regulation of cell cycle progression.

Two other published reports regarding *bcl*-2 and the cell cycle merit attention in this discussion. In the first (28), other investigators have found no differences in the in vivo labeling of $CD4^+8^+$ thymocytes from *bcl*-2 transgenic or control mice. It is difficult to reconcile these findings directly with ours. However, it is possible that no real differences exist between this study and ours, since the former was based upon a single transgenic animal during the period over which most DNA labeling occurs (3 d). In the second study (29), it has been suggested that *bcl*-2 expression can potentiate cell division in a multiply transfected hematopoietic cell line. The biological relevance of such a highly contrived system is difficult to assess. However, it is possible that the upregulation of *bcl*-2 seen after mitogenic stimulation in these cells is a protective response to allow cell cycle progression without inducing PCD, rather than a mandatory event in the induction of cell cycle progression; this is particularly true since the mitogenic stimulus in this case is IL-2. This explanation is also supported by the published findings of others, showing that growth factor receptor interaction is necessary to prevent PCD after the induction of proliferation (10).

In conclusion, our studies suggest that *bcl*-2 may regulate the progression of the cell division cycle in lymphoid cells (and possibly other tissue types) at a critical point where the decision between continued cell cycle progression or PCD is made. The prolongation of the cell division cycle at the G_1 to S phase transition may thus help to explain the well documented inhibition of PCD by *bcl*-2, by allowing additional time for the cell to prepare for DNA synthesis and/or repair DNA damage. The enhanced response of *bcl*-2 transgenic T cell cultures to in vitro stimuli (4) lends further support to such a concept. The biochemical determination of the upstream regulator(s) of the cell cycle that are affected by *bcl*-2 will allow further elucidation of this effect, and may reveal important clues regarding the connection between regulation of the cell division cycle and PCD in both normal and malignant cells.

The authors wish to thank Ms. Michelle Tourigny (Cornell University Graduate School of Medical Sciences) for assistance with cell sorting and review of the manuscript; Dr. Robert A. Schlegel (Pennsylvania State University) for critical review of the manuscript; Dr. Ken Shortman (Hall Institute, Melbourne) for consultation regarding in vivo labeling of thymocytes; Drs. David Vaux and Andreas Strasser (Hall Institute, Melbourne) for providing cell lines; Dr. Fritz Melchers (Basel Institute, Basel) for providing permission to use IL-3-producing cell lines; and Dr. David Tough (Scripps Institute, San Diego) for helpful discussions regarding BrdU labeling and detection.

This work was supported by research grant R29 AI 33940 from the National Institutes of Health (H.T. Petrie), by funds from the Special Projects Committee of the Society of Memorial Sloan-Kettering (H.T. Petrie), and by Cancer Center Support Grant NCI-P30-CA-08748 to the Memorial Sloan-Kettering Cancer Center.

Address correspondence to Howard T. Petrie, Memorial Sloan Kettering Cancer Center, Box 341, 1275 York Avenue, New York, NY 10021.

Received for publication 6 November 1995 and in revised form 4 March 1996.

References

1. Tsujimoto, Y., J. Cossman, E. Jaffe, and C.M. Croce. 1985. Involvement of the *bcl*-2 gene in human follicular lymphoma. *Science (Wash. DC).* 228:1440–1443.
2. Vaux, D.L., S. Cory, and J. Adams. 1988. Bcl-2 gene promotes hematopoietic cell survival and cooperates with c-*myc* to immortalize pre-B cells. *Nature (Lond.).* 335:440–442.
3. Sentman, C.L., L.R. Shutter, D. Hockenberry, O. Kanagawa, and S.J. Korsmeyer. 1991. *bcl*-2 inhibits multiple forms of apoptosis but not negative selection in thymocytes. *Cell.* 67:878–888.
4. Strasser A., A.W. Harris, and S. Cory. 1991. *bcl*-2 transgene inhibits T cell death and perturbs thymic self-censorship. *Cell.* 67:889–899.
5. Bissonnette, R.P., F. Echeverri, A. Mahboubi, and D.R. Green. 1992. Apoptotic cell death induced by c-*myc* is inhibited by *bcl*-2. *Nature (Lond.).* 359:552–554.
6. Fanidi, A., E.A. Harrington, and G.I. Evan. 1992. Cooperative interaction between c-*myc* and *bcl*-2 proto-oncogenes. *Nature (Lond.).* 359:554–556.
7. Hockenberry, D.M. 1995. *bcl*-2, a novel regulator of cell

death. *BioEssays*. 17:631–638.
8. Oltvai, Z.N., and S.J. Korsmeyer. 1994. Checkpoints of dueling dimers foil death wishes. *Cell*. 79:189–192.
9. Rubin, L., K.L. Philpott, and S.F. Brooks. 1993. The cell cycle and cell death. *Curr. Biol*. 3:391–394.
10. Evan, G.I., A.H. Wyllie, C.S. Gilbert, T.D. Littlewood, H. Land, M. Brooks, C.M. Waters, L.Z. Penn, and D.C. Hancock. 1992. Induction of apoptosis in fibroblasts by c-*myc* protein. *Cell*. 69:119–128.
11. Dedera, D.A., E.K. Waller, D.P. LeBrun, A. Sen-Majumder, M.E. Stevens, G.S. Barsh, and M.L. Cleary. 1993. Chimeric homeobox gene *E2A-PBX1* induces proliferation, apoptosis, and malignant lymphomas in transgenic mice. *Cell*. 74:833–843.
12. Haas-Kogan, D.A., S.C. Kogan, D. Levi, P. Dazin, A. T'Ang, Y-K.T. Fung, and M.A. Israel. 1995. Inhibition of apoptosis by the retinoblastoma gene product. *EMBO (Euro. Mol. Biol. Organ.) J*. 14:461–472.
13. Kowalik, T.F., J. DeGregori, J.K. Schwartz, and J.R. Nevins. 1995. E2F1 overexpression in quiescent fibroblasts leads to induction of cellular DNA synthesis and apoptosis. *J. Virol*. 69:2491–2500.
14. Yonish-Rouach, E., D. Resnitzky, J. Lotem, L. Sachs, A. Kimchi, and M. Oren. 1991. Wild-type p53 induces apoptosis of myeloid leukaemic cells that is inhibitable by IL-6. *Nature (Lond.)*. 352:345–347.
15. Miyashita, T., and J.C. Reed. 1995. Tumor suppressor p53 is a direct transcriptional activator of the human *bax* gene. *Cell*. 80:293–299.
16. Oltvai, Z.N., C.L. Milliman, and S.J. Korsmeyer. 1993. Bcl-2 heterodimerizes in vivo with a conserved homolog, Bax, that accelerates programmed cell death. *Cell*. 74:609–619.
17. Wang, E., M-J. Lee, and S. Pandey. 1994. Control of fibroblast senescence and activation of programmed cell death. *J. Cell Biochem*. 54:432–439.
18. Gazitt, Y., and G.W. Erdos. 1994. Fluctuations and ultrastructural localization of oncoproteins and cell cycle regulatory proteins during growth and apoptosis of synchronized AGF cells. *Cancer Res*. 54:950–956.
19. Meikrantz, W., S. Gisselbrecht, S.W. Tam, and R. Schlegel. 1994. Activation of cyclin A-dependent protein kinases during apoptosis. *Proc. Natl. Acad. Sci. USA*. 91:3754–3758.
20. Petrie, H.T., P. Hugo, R. Scollay, and K. Shortman. 1990. Lineage relationships and developmental kinetics of immature thymocytes: CD3, CD4, CD8 acquisition in vivo and in vitro. *J. Exp. Med*. 172:1583–1588.
21. Tough, D.F., and J. Sprent. 1995. Turnover of naive and memory-phenotype cells. *J. Exp. Med*. 179:1127–1135.
22. Karasuyama, H., and F. Melchers. 1988. Establishment of mouse cell lines which constitutively secrete large quantities of interleukin 2, 3, 4, or 5 using modified cDNA expression vectors. *Eur. J. Immunol*. 18:97–104.
23. Shortman, K., M. Egerton, G. Spangrude, and R. Scollay. 1990. The generation and fate of thymocytes. *Semin. Immunol*. 2:3–12.
24. Kato, J-Y, and C.J. Sherr. 1993. Inhibition of granulocyte differentiation by G_1 cyclins D2 and D3 but not D1. *Proc. Natl. Acad. Sci. USA*. 90:11513–11517.
25. Sherr, C.J., and J.M. Roberts. 1995. Inhibitors of mammalian G_1 cyclin-dependent kinases. *Genes & Dev*. 9:1149–1163.
26. Petrie, H.T., F. Livak, D. Burtrum, and S. Mazel. 1995. TCR gene recombination patterns and mechanisms: cell death, rescue, and T cell production. *J. Exp. Med*. 182:121–127.
27. Akbar, A.N., N. Borthwick, N. Salmon, W. Gombert, M. Bofill, N. Shamsadeen, D. Pilling, S. Pett, J.E. Grundy, and G. Janossy. 1993. The significance of low *bcl*-2 expression by CD45RO T cells in normal individuals and patients with acute viral infections. The role of apoptosis in T cell memory. *J. Exp. Med*. 178:427–438.
28. Siegal, R.M., M. Katsumata, M. Lang, J.C. Reed, and M.I. Greene. 1994. Repertoire selection and kinetics of T cell development in transgenic mice overexpressing *bcl*-2. *Transgenics*. 1:155–162.
29. Miyazaki, T., Z.J. Liu, A. Kawahara, Y. Minami, K. Yamada, Y. Tsujimoto, E.L. Barsoumian, R.M. Perlmutter, and T. Taniguchi. 1995. Three distinct IL-2 signaling pathways mediated by *bcl*-2, c-*myc*, and *lck* cooperate in hematopoietic cell proliferation. *Cell*. 81:223–231.